

## Crystal fields of $U^{3+}:\text{LaCl}_3$ under pressure

Th. Tröster\* and W. B. Holzapfel

*Fachbereich 6 Physik, Universität-GH-Paderborn, 33095 Paderborn, Germany*

J. Goffart

*Chimie Analytique et Radiochimie, B 16, Université Liege, Sart-Tilman, B-4000 Liege, Belgium*

(Received 26 August 1994)

Fluorescence and excitation spectra of  $U^{3+}:\text{LaCl}_3$  are presented for pressures up to 8 GPa and shifts of 27 energy levels are derived. Corresponding changes in the Slater parameters  $F^k$ , the spin-orbit coupling parameter  $\zeta$ , and the crystal-field parameters  $B_q^k$  are evaluated. The observed variations of the free-ion parameters  $F^k$  and  $\zeta$  are nearly an order of magnitude larger than in a former study on  $\text{Nd}^{3+}:\text{LaCl}_3$ . The behavior of the free-ion parameters is discussed in terms of different models. The crystal-field parameters are evaluated within the superposition model yielding intrinsic parameters  $\bar{B}_k(R)$  ( $k = 4, 6$ ). It is found that the distance dependence of the intrinsic parameters for  $U^{3+}:\text{LaCl}_3$  is nearly the same as in the case of  $\text{Nd}^{3+}:\text{LaCl}_3$ . Calculations using the angular-overlap model describe successfully the high-pressure results and indicate that the contact contributions to the crystal-field strength are the dominant terms.

### I. INTRODUCTION

Degenerate free-ion multiplets of lanthanides and actinides in ionic crystals are split by the crystal field. Although group theory predicts exactly the number of levels in which a given multiplet is split, it is much more difficult to calculate the actual magnitude of the splitting. Because different interactions between the  $f$  element and its surrounding are contributing to the crystal field strength, it is difficult to specify the relative weight of the various contributions.

Due to these difficulties the crystal field is usually described at first by a purely phenomenological one-electron potential, which often allows for a very good description of the crystal field levels. The reason for the success of this approach lies in the fact that it uses only symmetry arguments and makes no specific assumptions about the kind of interactions contributing to the crystal-field potential.<sup>1</sup> In a second step theoretical models like the superposition model<sup>2</sup> are used to describe the distance dependence of the crystal-field strength for a specific ligand. These models open also a simple way to compare experimental results with *ab initio* calculations.<sup>3,4</sup>

Besides the splitting of the free-ion multiplets in the crystal, the center of gravity of all multiplets shifts to the red. This redshift can be expressed as a reduction of the Slater and spin-orbit coupling parameters, which represent the Coulomb and spin-orbit interactions between the  $f$  electrons. At present a number of different models attempt to clarify these interactions both at ambient pressure<sup>5-8</sup> and high pressure,<sup>9-11</sup> but until now these models make quite different assumptions.

Therefore, high pressure offers a powerful tool to determine the kind and relative contributions of the various interactions responsible for both the free-ion parameter reduction and the crystal-field splittings. The continu-

ous variation of interatomic distances permits the direct determination of distance dependences of free-ion and crystal-field parameters. From the comparison of the experimental results with theoretical models it is then possible to test the predictions of the different models.

In previous investigations<sup>9,10</sup> the behavior of two lanthanide ions  $\text{Pr}^{3+}$  and  $\text{Nd}^{3+}$  in  $\text{LaCl}_3$  was studied under pressure. In the present work these investigations are extended to include the actinide ion  $U^{3+}$  in  $\text{LaCl}_3$ . Although the energy level structure of the  $U^{3+}$  ground configuration  $5f^3$  is formally equivalent to the  $\text{Nd}^{3+}$  ground configuration  $4f^3$ , there are some significant quantitative differences which can be attributed primarily to the larger radial extension of the  $5f$  wave function.

Due to smaller Coulomb interactions and larger spin-orbit coupling, deviations from  $LS$  coupling are much stronger in the case of  $U^{3+}$ . Moreover, the crystal-field splittings are about 2 times larger than for  $\text{Nd}^{3+}:\text{LaCl}_3$ ; therefore the effects of  $J$  mixing become much more important. Because of the stronger coupling to the lattice, the lines for  $U^{3+}$  become broader and vibronic sidebands are sometimes as strong as the purely electronic lines.

All these points complicate both the experimental and theoretical analyses for  $U^{3+}$ . A detailed description of the spectra and special features of  $U^{3+}:\text{LaCl}_3$  at ambient conditions has been given in the literature.<sup>12</sup>

### II. EXPERIMENTAL DETAILS

The fluorescence spectra of  $U^{3+}:\text{LaCl}_3$  were excited mostly with the 457 nm line of an argon-ion laser. In addition, excitation spectra were recorded with two different dyes, Rhodamin 6G and DCM, which allowed us to scan a region of more than  $2000\text{ cm}^{-1}$ .

The pressure was generated with a specially adapted

small diamond-anvil cell and determined by the ruby fluorescence method using the linear ruby scale<sup>13</sup> with constant thermal corrections.<sup>14</sup> All spectra were taken at temperatures of about 20 K, which were attained with a closed-cycled refrigerator. As the pressure transmitting medium, nitrogen was used.

The single crystals of  $\text{LaCl}_3$  were doped with 1 mol%  $\text{UCl}_3$ . All manipulations were carried out in a glove box under pure argon (water < 5 ppm, oxygen < 5 ppm).  $\text{UCl}_3$  was prepared by reaction of pure  $\text{HCl}$  on  $\text{UH}_3$  at 225 °C.  $\text{LaCl}_3$  freshly sublimated and  $\text{UCl}_3$  were grinded, mixed, and melted in a rotating furnace before slowly cooling (10 °C per minute) giving single crystals.

### III. RESULTS

#### A. Line shifts and energy levels

For the spectra at ambient pressure the assignment of the observed lines was adopted from the literature.<sup>12,15</sup> Due to the inhomogeneous broadening with increasing pressure, it was not possible to follow all lines to the maximum pressure of about 8 GPa. Nevertheless, 33 lines could be studied in all the fluorescence spectra.

Two typical fluorescence spectra at ambient pressure and 3.2 GPa are shown in Fig. 1. The fluorescence lines in this region can be assigned to the transition  ${}^2K_{15/2} \rightarrow {}^4I_{9/2}$ . The average line shift amounts to about 100  $\text{cm}^{-1}/\text{GPa}$ , which is nearly an order of magnitude larger than for  $\text{Nd}^{3+}$ . In contrast to this strong shift, the overall splitting of the ground state  ${}^4I_{9/2}$  of  $U^{3+}:\text{LaCl}_3$  shows only an increase similar to the case of  $\text{Nd}^{3+}:\text{LaCl}_3$ . The inhomogeneous broadening of the lines with increasing pressure is clearly visible; therefore, at higher pressures it is difficult to resolve some of the lines as for example lines *f* and *g*.

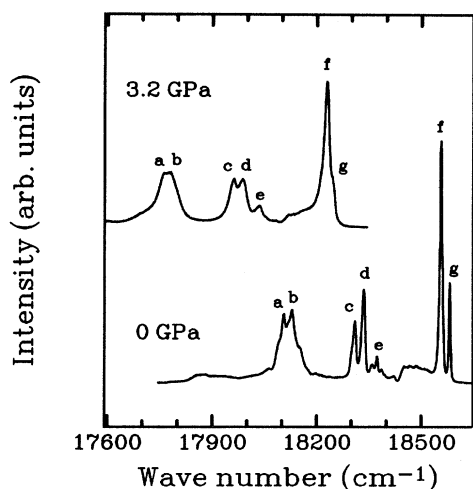


FIG. 1. Typical fluorescence spectra of  $U^{3+}:\text{LaCl}_3$  at ambient pressure and 3.2 GPa, both at 20 K. All lines can be assigned to the transition  ${}^2K_{15/2} \rightarrow {}^4I_{9/2}$ .

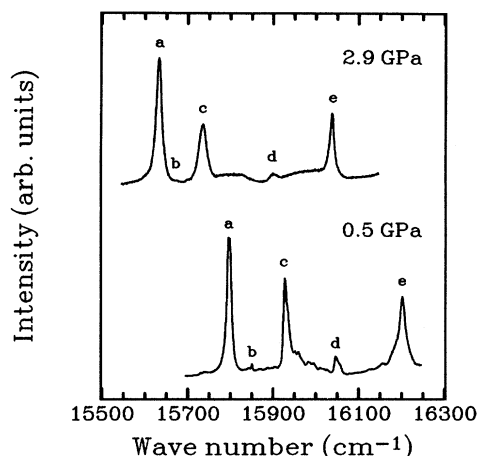


FIG. 2. Excitation spectra of  $U^{3+}:\text{LaCl}_3$  at 0.5 GPa and 3.2 GPa, both at 20 K. Lines *a* and *b* can be assigned to the transition  ${}^4I_{9/2} \rightarrow {}^2D_{3/2}$ , *c*, *d*, and *e* to  ${}^4I_{9/2} \rightarrow {}^2K_{13/2}$ .

Further information was obtained from the excitation spectra. Figure 2 shows two excitation spectra at 0.5 GPa and 2.9 GPa. However, due to the relative low temperature of 20 K, only transitions from the ground state were observed.

From both fluorescence and excitation spectra it is possible to derive the corresponding energy level shifts. Figure 3 shows the effect of pressure on five energy levels of the multiplets  ${}^2D_{3/2}$  and  ${}^2K_{13/2}$  as evaluated from the lines of Fig. 2. Altogether 27 energy levels were determined under pressure.

As illustrated in Fig. 3, the energy shifts can be decomposed into a shift of the center of gravity of the multiplets and a variation in the crystal field splittings. This approach is appropriate since the crystal fields of *f* elements in ionic crystals represent only a small perturbation of the free-ion multiplets.

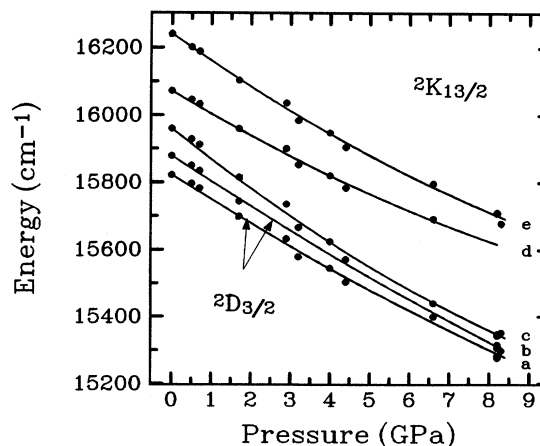


FIG. 3. Effect of pressure on the energy levels of the multiplets  ${}^2D_{3/2}$  and  ${}^2K_{13/2}$  of  $U^{3+}:\text{LaCl}_3$ .

## B. Parametric analysis

The Hamiltonian used to calculate the energy levels of  $U^{3+}:\text{LaCl}_3$  consists of two parts, one for the center of gravity of the free-ion multiplets and the other for the crystal-field splittings. Altogether 24 adjustable parameters are used to represent operators for the two-body electrostatic interaction ( $F^k$ ,  $k = 0, 2, 4, 6$ ), the two-body and three-body configuration interactions ( $\alpha$ ,  $\beta$ ,  $\gamma$ , and  $T^i$ ,  $i = 2, 3, 4, 6, 7, 8$ ), the spin-orbit interaction ( $\zeta$ ), the spin-spin and spin-other-orbit interactions ( $M^k$ ,  $k = 0, 2, 4$ ), the electrostatically correlated spin-orbit interaction ( $P^k$ ,  $k = 2, 4, 6$ ), and the crystal-field potential ( $B_0^2$ ,  $B_0^4$ ,  $B_0^6$ , and  $B_6^6$ ). A detailed discussion of the corresponding Hamiltonian can be found in the literature.<sup>16</sup>

The determination of all the parameters via a least squares fit is possible only if a sufficiently large data set is available. This is the case at ambient pressure, where 82 energy levels had been determined.<sup>12,15</sup> In contrast, the limited data set of 27 energy levels under pressure did not allow for independent determination of all the parameters; therefore only the Slater parameters  $F^k$ , the spin-orbit coupling parameter  $\zeta$ , the configuration-interaction parameters  $\alpha$  and  $\beta$ , and the four crystal-field parameters were fitted, keeping the other parameters fixed.

Besides the question of how many parameters can be fitted, it is of importance to know whether these parameters show a significant change in going from the larger data set known at ambient pressure (AP) to the reduced data set for high pressure (HP). Table I compares the parameters determined from the two different data sets at ambient pressure. It can be seen that the differences between the two sets are not larger than the statistical errors. Therefore, one can expect also that the variation of these parameters under pressure is accurately determined by the reduced data set.

### 1. Free-ion parameters

According to the strong redshift of the energy levels, the free-ion parameters show a pronounced decrease. As in the previous study on  $\text{Nd}^{3+}$  at first only the Slater and spin-orbit coupling parameters were varied. This leads in the present case to an increase of the standard deviation from  $30 \text{ cm}^{-1}$  at ambient pressure to  $57 \text{ cm}^{-1}$  at 8 GPa. Therefore it was necessary to vary also some of the other free-ion parameters. Since variations in the next two parameters for the configuration interaction,  $\alpha$  and  $\beta$ , already gave satisfactory results and the variation of the third configuration-interaction parameter  $\gamma$  did not give any further improvements,  $\gamma$  was fixed in all the later fits of high-pressure data.

It was then observed that the free-ion parameters changed nearly linearly with pressure. Table II gives the values of all these parameters at ambient pressure and at 8 GPa, together with their relative shifts in percent. As the main results one finds the following.

(1) The variation of the free-ion parameters is nearly an order of magnitude stronger for  $U^{3+}$  than for  $\text{Pr}^{3+}$  or  $\text{Nd}^{3+}$  in  $\text{LaCl}_3$ .

TABLE I. Free-ion and crystal-field parameters for  $U^{3+}:\text{LaCl}_3$  at ambient pressure (in  $\text{cm}^{-1}$ ) for two different data sets. Data set AP consists of 82 energy levels from the literature (Refs. 12, 15); the data set HP includes only the 27 energy levels observed under pressure. Parameters marked with an asterisk were not varied.

	(AP)	(HP)
$E_{\text{ave}}$	19554 (22)	19541 (11)
$F^2$	40047 (267)	39636 (156)
$F^4$	33611 (401)	33360 (327)
$F^6$	23610 (391)	23263 (269)
$\zeta$	1585 (5)	1593 (5)
$\alpha$	29 (1)	28 (1)
$\beta$	-793 (26)	-692 (62)
$\gamma$	904 (103)	904 (*)
$T^2$	146 (76)	146 (*)
$T^3$	60 (11)	60 (*)
$T^4$	248 (17)	248 (*)
$T^6$	-180 (30)	-180 (*)
$T^7$	575 (77)	575 (*)
$T^8$	334 (83)	334 (*)
$M_0$	0,67 (*)	0,67 (*)
$P^2$	1268 (69)	1268 (*)
$B_0^2$	306 (33)	340 (80)
$B_0^4$	-528 (101)	-551 (198)
$B_0^6$	-1352 (95)	-1497 (178)
$B_6^6$	1032 (66)	1079 (141)
$N$	82	27
$\sigma$	30	31

(2) Similar to the lanthanides, the variation of the Slater parameters decreases with  $k$ .

(3) The spin-orbit coupling parameter shows a significantly smaller variation with pressure than the Slater parameters, a behavior which was also found in the case of the lanthanides.

(4) The configuration-interaction parameters  $\alpha$  and  $\beta$  reveal a strong change with pressure. For  $\text{Nd}^{3+}$  and  $\text{Pr}^{3+}$ , on the other hand, it was possible to keep these parameters constant.

Since the third configuration-interaction parameter  $\gamma$  was not varied, it is possible that the variations of  $\alpha$  and

TABLE II. Free-ion parameters for  $U^{3+}:\text{LaCl}_3$  at ambient pressure and 8 GPa (in  $\text{cm}^{-1}$ ).

Parameter	0 GPa	8 GPa	$\Delta(\%)$
$E_{\text{ave}}$	19541 (11)	18870 (13)	-3.4 (1)
$F^2$	39636 (156)	37014 (259)	-6.6 (8)
$F^4$	33360 (327)	31594 (340)	-5.3 (1.4)
$F^6$	23263 (269)	22526 (344)	-3.2 (1.9)
$\zeta$	1593 (5)	1577 (9)	-1.0 (7)
$\alpha$	28 (1)	23 (1)	-17.0 (6)
$\beta$	-692 (62)	-460 (70)	+34.0 (14)
$N$	82	27	

$\beta$  are slightly overestimated, but in any case, a significant variation of  $\alpha$  and  $\beta$  remains. This effect can probably be attributed to a change in the energy difference between the  $5f^N$  ground configuration and excited configurations. In contrast to the lanthanides  $\text{Pr}^{3+}$  and  $\text{Nd}^{3+}$ , the relative changes are expected to be much larger for  $U^{3+}$ , since the ambient pressure differences are already considerably smaller and the crystal-field effects on the free-ion energies are in general much stronger in this case.

On the other hand, if one compares only the free-ion parameters  $F^k$  and  $\zeta$ , one may notice that both the lanthanides  $\text{Pr}^{3+}$  and  $\text{Nd}^{3+}$  and the actinide ion  $U^{3+}$  exhibit the same pressure dependences.

## 2. Crystal-field parameters

The effective  $D_{3h}$ -point symmetry at the site of the  $f$  elements in  $\text{LaCl}_3$  results in a crystal-field potential  $V$  that can be represented by only four real parameters  $B_q^k$ :

$$(|V|) = B_0^2 C_0^{(2)} + B_0^4 C_0^{(4)} + B_0^6 C_0^{(6)} + B_6^6 (C_6^{(6)} + C_{-6}^{(6)}).$$

The crystal-field splittings due to this potential are calculated by diagonalizing the energy matrix, where the matrix elements of the tensor operators  $C_q^{(k)}$  depend on the free-ion eigenvectors and can be calculated exactly. In the case of the former studies on  $\text{Pr}^{3+}$  and  $\text{Nd}^{3+}$  these eigenvectors showed no significant change under pressure;

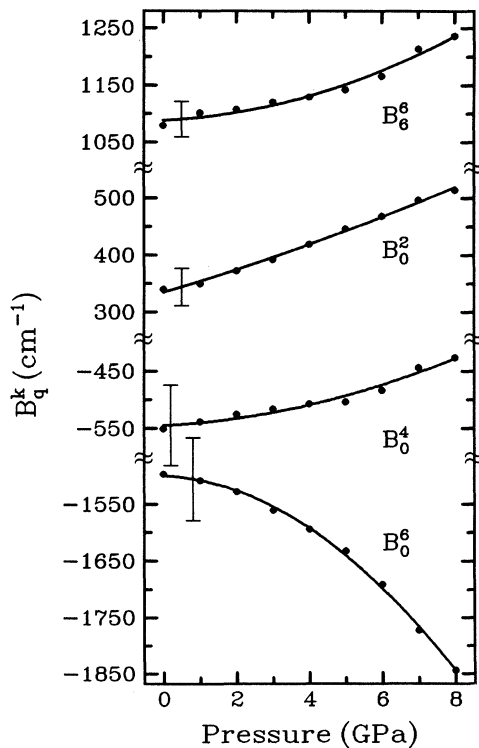


FIG. 4. Effect of pressure on the crystal-field parameters  $B_0^{2,4,6}$  and  $B_6^6$  for  $U^{3+}:\text{LaCl}_3$ .

thus it was possible to use the same matrix elements at each pressure. In contrast, due to the strong variation of the free-ion parameters in the case of  $U^{3+}:\text{LaCl}_3$  also the composition of some eigenvectors change dramatically (up to 30%). Therefore, it was necessary to repeat the calculation of the matrix elements of the tensor operators at each pressure.

The variation of the crystal-field parameters  $B_q^k$  with pressure is shown in Fig. 4. In comparison with former results on the lanthanides one can notice the following facts.

(1) The magnitude of  $B_0^4$  decreases as in the case of the lanthanides, though the overall shift is a factor of 2 larger.

(2) The absolute values of both  $B_0^6$  and  $B_6^6$  increase with pressure. Not only the qualitative behavior, but also the relative shifts are similar to the lanthanides.

(3) In contrast to  $\text{Pr}^{3+}$  and  $\text{Nd}^{3+}$  a simple increase is observed for  $B_0^2$ , which amounts to about 50% at 8 GPa.

## IV. DISCUSSION

### A. Free-ion models

The reduction of the free-ion parameters in crystals has been ascribed to different mechanisms, where in general two types of models can be distinguished. On the one hand, one has the wave function renormalization or covalent models, which consider an expansion of the open-shell orbitals in the crystal. This expansion follows either from a covalent admixture with ligand orbitals or from a modification of the effective nuclear charge, due to the penetration of the ligand electron clouds into the metal ion. On the other hand, electrostatic models regard the whole crystal or even the ligands as polarizable units and thereby lead to weaker Coulomb and spin-orbit interactions.

The modification of the effective nuclear charge  $Z^*$  predicts, for the change in the free-ion parameters,<sup>17</sup>

$$\Delta F^k \sim Z^* \quad \text{and} \quad \Delta \zeta \sim Z^{*3}.$$

Thus the variation of the spin-orbit coupling parameter should be much stronger than for the Slater parameters. On the contrary, the present high-pressure results for  $\text{Pr}^{3+}$ ,  $\text{Nd}^{3+}$ , and  $U^{3+}$  reveal that the variation of the spin-orbit coupling parameter is clearly weaker than the variation of the Slater parameters. Therefore, it is certainly not possible to describe the high-pressure results only by a variation of the effective nuclear charge.

On the other hand, the covalent admixture of the  $f$  orbitals with ligand orbitals leads to

$$\Delta F^k \sim N^4 \quad \text{and} \quad \Delta \zeta \sim N^2,$$

where  $N$  is a renormalization coefficient, expressible as a sum including overlap integrals and covalency parameters.<sup>8</sup> Indeed, this mechanism can explain the stronger variation of the Slater parameters with respect to the spin-orbit coupling parameter under pressure.

However, *ab initio* calculations<sup>18</sup> have shown that this effect is too weak to account for the observed reduction of the free-ion parameters at least in the case of the lanthanides. Therefore, this mechanism alone cannot explain the reduction and other mechanisms must be invoked.

One additional effect of the crystalline environment is the screening of the Coulomb interaction due to the fact that the crystal can be treated as a dielectric continuum or polarizable medium. This mechanism was first proposed for  $3d$  ions<sup>19</sup> and it was shown, that also in the case of  $f$  elements such models can predict Slater parameter shifts of the order of magnitude observed experimentally.<sup>7</sup>

According to the dielectric model<sup>19</sup> the  $f$  element is placed within an empty sphere with radius  $R_S$ . Embedding the sphere into an infinite medium with dielectric constant  $\epsilon$  leads to a reduction  $\Delta F^k$  of the Slater parameters:<sup>7</sup>

$$\Delta F^k = \frac{(\epsilon - 1)\langle r^k \rangle^2}{\left(\frac{k}{k+1} + \epsilon\right)R_S^{2k+1}}.$$

The main problem here is related to the definition of the radius  $R_S$ . It is assumed that  $R_S$  is proportional to the mean  $U^{3+}\text{-Cl}^-$  distance  $\bar{R}$  under pressure, determined from the nine nearest neighbors, six of these at distances  $R_A$  and three at  $R_E$ :

$$R_S \sim \bar{R} = \frac{1}{9}(6R_A + 3R_E).$$

Since the absolute values for  $R_S$  at ambient condition are free parameters in this model, one can adopt best fitting values for the ratios  $R_S/\bar{R}$  of 0.424 for  $\text{Pr}^{3+}$ , 0.417 for  $\text{Nd}^{3+}$ , and 0.500 for  $U^{3+}$ , which then reproduce the high-pressure results for  $\Delta F^6$  exactly and give also reasonable values in the other cases as shown in Table III.

It must be emphasized that both the absolute values for the  $\Delta F^k$  and also the ratios  $\Delta F^{k+2}/\Delta F^k$  depend strongly on the choice of  $R_S$  at ambient pressure. Nevertheless, it can be seen from Table III that this simple model produces shifts that are at least of the correct order of magnitude.

## B. Superposition model

The superposition model (SM) was developed to separate the angular and radial dependences in crystal field

TABLE III. Experimental results for the Slater parameter reductions of  $\text{Pr}^{3+}$ ,  $\text{Nd}^{3+}$ , and  $U^{3+}$  in  $\text{LaCl}_3$  under pressure in comparison with results from the dielectric model. All values in  $\text{cm}^{-1}$ .

Parameter	$\text{Pr}^{3+}$		$\text{Nd}^{3+}$		$U^{3+}$	
	Expt.	Calc.	Expt.	Calc.	Expt.	Calc.
$\Delta F^2$	-683	-323	-477	-298	-2622	-659
$\Delta F^4$	-398	-129	-204	-109	-1766	-435
$\Delta F^6$	-198	-195	-155	-150	-737	-750

parameters.<sup>2,1</sup> The basis of the model lies in the assumption that the crystal field is additive and can be built up from the contributions of individual ligands, where interactions between the ligands are ignored. In general only the nearest neighbors are taken into account.

Within the SM the number of crystal-field parameters  $B_q^k$  is reduced further, because all the parameters with the same  $k$  but different  $q$  can be expressed by only one intrinsic parameter  $\bar{B}_k$ . The new intrinsic parameters depend only on the kind of the ligands and their distance  $R$  to the  $f$  element. For the crystal-field parameters  $B_q^k$  and the intrinsic parameters  $\bar{B}_k$  one obtains the relation

$$B_q^k = \sum_N \bar{B}_k(R_N) K_{kq}(\Theta_N, \Phi_N) \alpha_{k0} / \alpha_{kq}.$$

Here the sum runs over the  $N$  nearest neighbors at distances  $R_N$ . The coordination factors  $K_{kq}$  depend only on the angular coordinates  $\Theta_N$  and  $\Phi_N$ . Together with the coefficients  $\alpha_{kq}$  they are given in Ref. 20. For the distance dependence of the intrinsic parameters  $\bar{B}_k$  usually a simple power law is used:

$$\bar{B}_k(R) = \bar{B}_k(R_0) \left(\frac{R_0}{R}\right)^{t_k},$$

where  $R_0$  is a reference distance, which is selected here to be equal to the ambient pressure distance in  $\text{LaCl}_3$ . To deduce the intrinsic parameters  $\bar{B}_k(R_0)$  and the distance dependence represented by the exponents  $t_k$ , it is necessary to know the variations of the bond angles and distances between the  $U^{3+}$  impurity ion and its ligands under pressure. Because the ionic radius of  $U^{3+}$  is very similar to that of  $\text{La}^{3+}$  in  $\text{LaCl}_3$ , local distortions can be neglected and the same changes as around the  $\text{La}^{3+}$  ion in the host crystal<sup>10</sup> should be expected.

The intrinsic parameters  $\bar{B}_4(R)$  and  $\bar{B}_6(R)$  were determined from the crystal-field parameters  $B_4^4$ ,  $B_6^6$ , and  $B_6^6$  of  $U^{3+}:\text{LaCl}_3$ . The results are summarized in Table IV. For comparison, also the intrinsic parameters of  $\text{Pr}^{3+}$  and  $\text{Nd}^{3+}$  in  $\text{LaCl}_3$  are shown. The values are not identical with the data in Ref. 10, because slightly different local distortions around  $\text{Pr}^{3+}$  and  $\text{Nd}^{3+}$  were used in the present case. Nevertheless, the deviations are within the statistical error.

As can be seen from the intrinsic parameters in Table IV, the crystal-field strength for  $U^{3+}$  at ambient pressure, represented by  $\bar{B}_k(R_0)$ , shows about twice the value of the lanthanides. In spite of this remarkable difference,

TABLE IV. Intrinsic parameters  $\bar{B}_{4,6}(R_0)$  (in  $\text{cm}^{-1}$ ) and power law exponents  $t_{4,6}$  for  $\text{Pr}^{3+}$ ,  $\text{Nd}^{3+}$ , and  $U^{3+}$  in  $\text{LaCl}_3$ .  $R_0 = 295$  pm.

	$\bar{B}_4(R_0)$	$t_4$	$\bar{B}_6(R_0)$	$t_6$
$\text{Pr}^{3+}$	287 (22)	5 (4)	258 (28)	7 (2)
$\text{Nd}^{3+}$	254 (28)	2 (4)	271 (32)	6 (2)
$U^{3+}$	507 (47)	7 (4)	585 (52)	5 (2)

TABLE V. Intrinsic parameters  $\bar{B}_{4,6}(R_0)$  (in  $\text{cm}^{-1}$ ) and power law exponents  $t_{4,6}$  for  $U^{3+}$  in  $\text{LaCl}_3$ . The AOM values are calculated from parameters given in Ref. 23.  $R_0 = 295$  pm.

	$\bar{B}_4(R_0)$	$t_4$	$\bar{B}_6(R_0)$	$t_6$
AOM	826	6	468	4
SM	507 (47)	7 (4)	585 (52)	5 (2)

the distance dependences are nearly the same in all cases. The apparent difference in the case of  $t_4$  for  $\text{Nd}^{3+}:\text{LaCl}_3$  is most probably due to uncertainties in the determination of the local distortions.<sup>10</sup>

The good agreement obtained by comparing the experimental results for the intrinsic parameters of  $\text{Pr}^{3+}$  and  $\text{Nd}^{3+}$  in  $\text{LaCl}_3$  with *ab initio* calculations emphasized the importance of contact contributions to the crystal field strength.<sup>4</sup> In the case of  $U^{3+}$  these contributions should be even more important due to the larger radial extension of the  $f$  electrons. Therefore, the angular overlap model<sup>21,22</sup> (AOM) should provide also a good description of the experimental results.

In the AOM the dominant contributions to the crystal field are described by the parameters  $e_\sigma$  and  $e_\pi$ . These parameters can be related to the intrinsic parameters by simple relations.<sup>23</sup> The AOM parameters can be written also with the same power law forms as the intrinsic parameters. Therefore, the distance dependences are described by parameter values  $e_\mu(R_0)$  ( $\mu = \sigma, \pi$ ) at the reference distance  $R_0$  and exponents  $\alpha_\mu$ . In the case of  $\text{UCl}_3$  the ambient pressure values  $e_\mu(R_0)$  had been already determined experimentally<sup>24</sup> and in addition the exponents  $\alpha_\mu$  had been evaluated from calculations of overlap integrals.<sup>23</sup>

With these data, the intrinsic parameters (AOM) in Table V were calculated. It is obvious that the AOM can successfully describe the high-pressure results evaluated within the SM, again indicating the importance of contact contributions to the crystal field. Only in the case of  $\bar{B}_4(R_0)$  a significant deviation is observed. This deviation is reduced if a third AOM parameter  $e_\delta$ , also given in Refs. 24, 23, is taken into account. This parameter describes nonaxial ligand interactions, which are not included in the SM.<sup>20</sup> In that case, one obtains  $\bar{B}_4(R_0) = 736 \text{ cm}^{-1}$  and  $\bar{B}_6(R_0) = 501 \text{ cm}^{-1}$ , whereas the exponents are not changed.

## V. CONCLUSIONS

From fluorescence and excitation spectra it was possible to determine 27 energy levels of  $U^{3+}:\text{LaCl}_3$  under pressure. The shifts of the energy levels are described by changes in the free-ion parameters  $F^k$ ,  $\zeta$ ,  $\alpha$ , and  $\beta$  and in the crystal-field parameters  $B_q^k$ . It is found that the variations of the free-ion parameters are nearly an order of magnitude larger than in the case of a former study on  $\text{Nd}^{3+}:\text{LaCl}_3$ . Nevertheless, the qualitative behavior is similar.

From the comparison of the variation of the free-ion parameters with different models it follows that the central field covalency is not able to describe the experimental results. While the mixing with ligand orbitals reproduces at least the qualitative behavior, *ab initio* calculations show that this mechanism alone cannot account for the observed shifts.<sup>18</sup> However, since a simple electrostatic model describes the reduction of the Slater parameters reasonably, one can assume that electrostatic interactions play an important role.

The crystal-field parameters were evaluated in the frame of the superposition model, yielding intrinsic parameters  $\bar{B}_{4,6}(R)$ . It was shown that the distance dependences ( $t_k$ ) for  $U^{3+}$  and  $\text{Nd}^{3+}$  in  $\text{LaCl}_3$  are almost the same, even though the absolute values at ambient conditions are quite different. Calculations in the frame of the angular overlap model describe the experimental results and indicate that contact effects are important for the crystal-field splittings.

In summary the present high-pressure studies point to the possibility that the reduction of the free-ion parameters is strongly influenced by electrostatic interactions, whereas contact effects seem to dominate in the case of the crystal-field splittings. With the assumption of different physical mechanisms for the free-ion parameter reduction and the crystal field splittings, it seems possible to explain the anticorrelation of the nephelauxetic<sup>25</sup> and the spectrochemical<sup>26</sup> series (see Ref. 8), which orders the ligands of  $f$  elements with respect to increasing free-ion parameter shifts and increasing crystal-field splittings, respectively.

## ACKNOWLEDGMENT

This work was supported by the Deutsche Forschungsgemeinschaft (DFG) under Grant No. Ho486/14.

\* Present address: Universidade Estadual de Campinas, Instituto de Física, C.P. 1170, 13083-970 Campinas, SP, Brazil.

<sup>1</sup> D.J. Newman, *Adv. Phys.* **20**, 197 (1971).

<sup>2</sup> M.I. Bradbury and D.J. Newman, *Chem. Phys. Lett.* **1**, 44 (1967).

<sup>3</sup> D.J. Newman and Betty Ng, *J. Phys. C* **19**, 389 (1986).

<sup>4</sup> Y.R. Shen and W.B. Holzapfel, *J. Phys. Condens. Matter* **6**, 2367 (1994).

<sup>5</sup> C.K. Jørgensen, *Orbitals in Atoms and Molecules* (Academic Press, New York, 1962).

<sup>6</sup> R. Reisfeld and Chr.K. Jørgensen, *Lasers and Excited States of Rare Earths*, Inorganic Chemical Concepts 1 (Springer-Verlag, Berlin, 1977).

<sup>7</sup> D.J. Newman, *J. Phys. Chem. Solids* **34**, 541 (1973).

<sup>8</sup> D.J. Newman, Betty Ng, and Y.M. Poon, *J. Phys. C* **17**, 5577 (1984).

<sup>9</sup> T. Gregorian, H. d'Amour-Sturm, and W.B. Holzapfel,

- Phys. Rev. B **39**, 12 497 (1989).
- <sup>10</sup> Th. Tröster, T. Gregorian, and W.B. Holzapfel, Phys. Rev. B **48**, 2960 (1993).
- <sup>11</sup> Qiuping Wang and Alain Bulou, J. Phys. Condens. Matter **5**, 7657 (1993).
- <sup>12</sup> H.M. Crosswhite, H. Crosswhite, W.T. Carnall, and A.P. Paszek, J. Chem. Phys. **72**, 5103 (1980).
- <sup>13</sup> G.J. Piermarini, S. Block, J.D. Barnett, and R.A. Forman, J. Appl. Phys. **46**, 2774 (1975).
- <sup>14</sup> R.A. Noack and W.B. Holzapfel, in *High Pressure Science and Technology*, edited by K.D. Timmerhaus and M.S. Barber (Plenum, New York, 1979), Vol. 1, p. 748.
- <sup>15</sup> W.T. Carnall (unpublished).
- <sup>16</sup> H.M. Crosswhite, H. Crosswhite, F.W. Kaseta, and R. Sarup, J. Chem. Phys. **64**, 1981 (1976).
- <sup>17</sup> Z.B. Goldschmidt, in *Atomic Properties (Free Atom)*, Handbook on the Physics and Chemistry of Rare Earths, edited by K.A. Gschneidner, Jr. and L. Eyring (North-Holland, Amsterdam, 1978).
- <sup>18</sup> Betty Ng and D.J. Newman, J. Chem. Phys. **87**, 7110 (1987).
- <sup>19</sup> C. Morrison, D.R. Mason, and C. Kikuchi, Phys. Lett. **24A**, 607 (1967).
- <sup>20</sup> D.J. Newman and Betty Ng, Rep. Prog. Phys. **52**, 699 (1989).
- <sup>21</sup> C.K. Jørgensen, R. Pappalardo, and H.H. Schmidtke, J. Chem. Phys. **39**, 401 (1965).
- <sup>22</sup> C.E. Schäffer, Struct. Bonding **5**, 68 (1968).
- <sup>23</sup> Z. Gajek and J. Mulak, J. Phys. Condens. Matter **4**, 427 (1992).
- <sup>24</sup> Z. Gajek and J. Mulak, J. Solid State Chem. **87**, 218 (1990).
- <sup>25</sup> C.E. Schäffer and Chr.K. Jørgensen, J. Inorg. Nucl. Chem. **8**, 143 (1958).
- <sup>26</sup> J.S. Griffith, *The Theory of Transition Metal Ions* (Cambridge University Press, Cambridge, England, 1961).